Solution and Solid State Study of Nickel(II) Ternary Complexes Containing 5-Aminolevulinic Acid Drug and Amino Acids

Salhah D. Al-Qahtani[iD]

Department of Chemistry, College of Science, Princess Nourah bint Abdulrahman University, Riyadh, Saudi Arabia

Corresponding author: E-mail: sdalohtany@pnu.edu.sa

Solution equilibria of the systems Ni(II)-5-aminolevulinic acid as ligand (A) and the amino acids [alanine (Ala), valine (Val), methylamine (Met), imidazole (Imi), Histidine (His), serine (Ser), cysteine (Cys) and penicillamine (Pen)] as ligands (L) have been studied pH-metrically. The stability constants of mixed ligand complexes were calculated with I = 0.10 mol L^{-1} KNO$_3$ using HYPERQUAD program at 25 ± 0.1 °C. The log10 X values showed a higher stabilities for the mixed ligand complexes compared to the binary analogues. The synthesis and characterization of the new amino acid mononuclear Ni(II) binary complex [NiA] (**1**) and ternary complex [NiAL] (**2**) were achieved *via* molar conductance, elemental analysis UV-vis, IR, ^{1}H NMR, thermal analysis and magnetic moment. The thermogravimetric analysis of complexes were investigated by TG-DTA suggests that the complexes possess high thermal stability formation and their respective nickel oxide for **1** and nickel sulfide for **2** as final chemical entities, which are thermally stable. The nickel(II) chelates were found to be non-electrolytes, diamagnetic moments and the geometry around Ni(II) ion in complexes **1** and **2** is square planar.

Keywords: Ni(II) complexes, Potentiometric studies, Amino Acids, 5-Aminolevulinic acid, Mixed ligand complexes.

INTRODUCTION

Investigations of metal complexes′ drug interactions have been initiated due to their improved curative effects, which are involved in developing medicinal and biotechnological novel reagents. The drugs efficiency in coordination with a metal is enhanced in several cases [1]. The metal containing drugs can adjust ligands in a three-dimensional configuration precisely, which enables the accommodation of the molecule to identify and interact with a particular molecular target. This is additionally advanced by the various chemical modifications of ligands. Furthermore, metal complexes undergo ligand substitution and redox reactions readily, allowing them to interact with biological molecules and participate in biological redox chemistry [2-4]. Multiple complexes have antifungicidal, antiviral, antibacterial and anticancer bioactivity and have been determined to be more antimicrobial than their ligands [5]. Recently, significant attention has been regarded to mixed chelation due to its wide occurrence in bio-fluids, where there is a significant number of potential ligands prone to competition for the metal ions present *in vivo* [6,7]. In various biological

processes, ternary coordination complexes are perceived to have a vital function, for example in the process of enzyme activation by metal ions [6].

Mixed-ligand complexes are also involved in active substances′ transport and storage, which occurs through membranes. Therefore, there is great reliance of such phenomenon on metal ions' configuration and the formation of these species. Ternary complexes of metal(II) that contain oxygen-donor and nitrogen ligands have gained much attention as they can demonstrate outstanding stability [8-10]. Ternary metal complexes have been investigated due to their ability as metal systems for metal-protein complexes, such as metalloenzymes. They received particular recognition and have been assigned to map protein surfaces, [11] as probes for biological redox centers [12] and in protein capture for both refinement [13] and examination [14,15]. Drugs and amino acids have notable medicinal and biological importance; therefore, the attention has been recently paid to the study of ternary complexes of transition metals with molecules of pharmaceutical and biological interest. Aminolevulinic acid (A) is a metabolic pro-drug that is converted into the photosensitizer protoporphyrin IX (PpIX), which expands

intracellularly. When exposed to light of suitable wavelength (red or blue), oxygen catalyzes to singlet oxygen by PpIX, which is an intracellular toxin that can subsequently react to produce hydroxyl radicals and superoxide. This results in cellular cyto-toxic effects. Moreover, it was reported that a complex of iron and aminolevulinic acid can incite murine hair growth *in vivo* independent of mesenchymal and epithelial cells. Accordingly, this complex has the potential to be a new beneficial remedy for the treatment of alopecia [16]. The present study reported the formation of binary and mixed ligand complexes of Ni(II) with selected L-amino acids and 5-amino-levulinic acid drug by potentiometric titration technique in aqueous medium at 25 ± 0.1 ºC with I = 0.10 mol L^{-1} KNO$_3$. The isolated metal chelates, [NiA] and [NiAL] are distinguished by molar conduc-tance, magnetic moments, elemental analyses, IR electronic, ^{1}H NMR spectral measurements and TG/DTA analysis.

EXPERIMENTAL

The preparation of all experimental solutions was in ultra-pure water with 18.3 mol L^{-1} Ω cm resistivity. All the ligands used were extra pure ranged from 99-99.9% Sigma products. Moreover, 0.005 mol L^{-1} nickel solution used in this study was provided by BDH as nitrate salt of Ni(NO$_3$)$_2$·6H$_2$O was checked by EDTA titration [17]. In order to determine the stability constant, two equivalents of HNO$_3$ acid were used for the preparation of aminolevulinic acid solution. CO$_2$ free NaOH, which is a titrant prepared in 0.1 mol L^{-1} KNO$_3$ solution was standardized using potassium hydrogen phthalate pH-metrically [18]. Carlo-Erba 1106 elemental analyzer was employed to analyze nitrogen, hydrogen and carbon. Moreover, the use of Kjeldahl′s method was used to assess the determination of Ni(II) chelates′ nitrogen content. Furthermore, data from Ni(II) chelates′ electronic spectra were obtained from the Shimadzu Model 1601 UV-Visible Spectrophotometer. In addition, KBr pellets were used in order to record FT-IR spectra on a FTIR-Shimadzu model IR-Affinity-1 spectrophotometer. Finally, EI technique allowed the recording of the mass spectra with the use of MS-5988 GS-MS Hewlett-Packard instrument at 70 eV. Using the internal reference TMS, JEOL JNM-ECZ500R/S1 FT NMR spectrometer recorded ^{1}H NMR spectra of nickel chelates.

Synthesis of binary nickel(II) chelate: The dissolution of 1.31 g; 1 mmol of 5-aminolevulinic acid (A) in ethanol (20

mL). Furthermore, dissolution of Ni(NO$_3$)$_2$·6H$_2$O (1.62 g; 1 mmol) in 20 mL ethanol, which was added dropwise. Furthermore, stirring of the mixture was performed for 3 h at 60 ºC.

For the purpose of solid formation, the solvent was given time to evaporate in a slow manner. Subsequently, filtration was used to collect the solid produced and the substance was then washed using diethylether and ethanol to achieve the complex in its pure form (**Scheme-I**). Colour: reddish brown; yield: 63%; m.p.: 138 ºC; Elemental analysis of C$_5$H$_{10}$N$_2$O$_7$Ni found (calcd.) % (m.w. = 268.8): Ni = 21.77 (21.83), C = 19.39 (19.42), H = 3.72 (3.75), N = 10.36 (10.42); μ$_{eff}$(B.M.) = 0.2 (diamagnetic); Λ$_m$ = 2.36 Ω^{-1} mol^{-1} cm^2.

Synthesis of ternary nickel(II) chelate: In a 20 mL of hot ethanol, an appropriate amount of Ni(NO$_3$)$_2$·6H$_2$O (1.62 g, 1 mmol) was dissolved. Furthermore, an addition of 20 mL of boiling ethanoic solution of 5-aminolevulinic acid (A) (1.31 g; 1 mmol) was prepared followed by the addition of cysteine (1.21 g, 1 mmol). First, the mixture was heated in a water bath for 3 h before its filtration. The resultant filtrate generated dark, shiny green crystals when left overnight. Furthermore, the crystals produced were filtered and washed with diethyl ether and ethanol to obtain the required complex (**Scheme-I**). Colour: deep brown; yield 85 %, m.p.: >300 ºC; Elemental analysis of C$_8$H$_{14}$N$_2$O$_5$SNi (m.w. = 309) found (clacd) %: Ni = 18.87 (19.00), C = 30.97 (31.10), H = 4.51 (4.57), N = 8.96 (9.07), S = 10.29 (10.38); μ$_{eff}$ (B.M.) =0.2 (diamagnetic); Λ$_m$ = 4.82 Ω^{-1} mol^{-1} cm^2.

pH Measurements: Griffin pH J-300-010 G Digital pH meter was utilized to obtain potentiometric measurements at 25 ± 0.1 ºC and an ionic strength of 0.10 mol L^{-1} KNO$_3$. Titra-tions of the mixed ligand systems were carried out on aliquots (40 mL) of solution containing 0.005 mol L^{-1} of the corres-ponding Ni(II), amino acid and A ligands (L) in 1:1:1 ratio with known volume of standard CO$_2$ free NaOH. In a nitrogen atmosphere at I = 0.1 mol L^{-1} KNO$_3$ was used, where all titrations were performed, in addition to use 0.05 mol L^{-1} NaOH as a titrant. In order to ensure the complete protonation at the start of the experiment, an addition of HNO$_3$ solution was made. To check the accuracy of data obtained, the conduction of the titration of all sets took place four times.

In order to measure the formation constants of metal complexes and their proton association based on potentiometric data, the Hyperquad program was used [19]. Consequently,
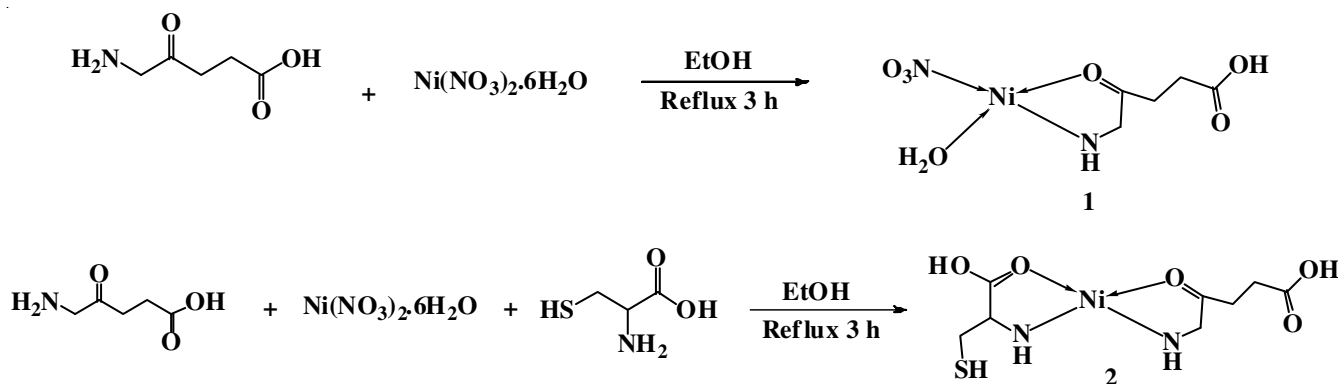
Scheme-I: Synthetic methods of chelate **1** and **2**

based on the non-linear least-square sum minimization, a fitting criterion was established. The difference between the experimental and calculated data of the titration curves defines the minimization (eqn. 1):

$$X^2 = \sum \frac{(\text{Calculated} - \text{Experimental})^2}{\text{Experimental}} \quad (1)$$

These constants were presented as the overall formation constant (β_{lpqr}) with stoichiometric coefficients l, p, q and r that represent Ni(II) ion, A, L and proton, in the order given. The function of the formation constant is defined as the concentration of free reactants [H], [A], [L] and [Ni], in addition to the concentration of the complex species $[Ni_lA_pL_qH_r]$, which can be estimated using the equation bellow:

$$l(Ni) + p(A) + q(L) + r(H) \rightleftharpoons (Ni)_l (A)_p (L)_q (H)_r \quad (2)$$

$$\beta_{lpqr} = \frac{[Ni_lA_pL_qH_r]}{\{[Ni]^l[A]^p[L]^q[H]^r\}} \quad (3)$$

The concentration curves of complex species represented graphically are presented by a HySS program distribution diagram [20].

RESULTS AND DISCUSSION

Solution equilibrium studies: The protonation constants of the amino acids ligands were determined under the above experimental conditions, which allowed the determination of Ni(II) complexes′ formation constants. Furthermore, the data in the literature are consistent with the estimated data [21-23]. The determined values of mixed ligand species found in Ni(II)-A-L systems, which are constants of formation, binary stability and proton association are shown in Table-1.

To determine the formation constants of Ni(L) and Ni(A) complexes, the potentiometric data was imposed on the basis of the models of possible composition. Consequently, it was found that the most statistically fit model consists of NiL (1010), NiL$_2$ (1020), Ni(A) (1100) and Ni(A)$_2$ (1200) complexes (Table-1).

The mixed ligand complexes associated with amino acids and drugs demonstrate titration data that comply with the formation of species, such as NiL, NiL$_2$, Ni(A), Ni(A)(L), Ni(A)(LH) and Ni(A)$_2$. Imidazole complexes and monodentate compounds methylamine have formation constants that are relatively lower than those of amino acid complexes as shown in Table-1, which demonstrated the bidentate ligand function of amino acids, which coordinate through the carboxylate and amino groups. Methylamine complex has a higher constant value of formation in comparison to the formation constant value of an imidazole complex, which might be a result of the amino group in imidazole that leads to greater basicity (demonstrated by pK_a values).

The equation below determines the value of the protonated species′ acid dissociation constants:

$$pK_{Ni(A)L}^H = \log K_{Ni(A)(L)H}^{Ni(A)} - \log K_{Ni(A)(L)}^{Ni(A)} \quad (4)$$

It is shown that histidine is capable of forming complex species that are deprotonated (1110) and protonated (1111).

5.58 is the pK_a value for the histidine complex, which is lower than the pK_a value of 9.85 assigned to the histidine ligand protonated amino group (-NH$_3^+$). However, it is close to the pK_a of protonated imidazole, which is 6.12. As a consequence of complex formation, an increase of acidity was observed, which indicates that the imidazole group is the main location of the protonated complex proton.

The acid dissociation constants of the protonated ternary complex obtained with thiol-containing ligands as penicillamine and cysteine were 7.43 and 5.08, respectively. These values obtained in the present study were less than the previously reported [24], revealing that [-NH$_3^+$] and -SH groups most likely participate in the formation of a complex.

A comparison was made between the formation constants of $\log_{10} K_{Ni(A)(L)}^{Ni(A)}$ and $\log_{10} K_{Ni(A)(L)}^{Ni(L)}$ to know which ligand acts as a primary and a secondary ligand, in addition to deciding which one is involved in forming mixed ligand complexes, eqns. 5 and 6 were used for this purpose.

$$\log_{10} K_{Ni(A)(L)}^{Ni(A)} = \log_{10} \beta_{Ni(A)(L)}^{Ni} - \log_{10} K_{Ni(A)}^{Ni} \quad (5)$$

$$\log_{10} K_{Ni(A)(L)}^{Ni(L)} = \log_{10} \beta_{Ni(A)(L)}^{Ni} - \log_{10} K_{Ni(L)}^{Ni} \quad (6)$$

$\log_{10} K_{Ni(A)(L)}^{Ni(A)}$ and $\log_{10} K_{Ni(A)(L)}^{Ni(L)}$ constants were calculated for each mixed ligand system as shown in Table-1. Upon consideration of other ligands and the drug potential, the formation of ternary complexes can progress through a simultaneous mechanism or stepwise. It is observed in all systems that amino acids act as the secondary ligands, while 5-aminolevulinic acid acts as the primary ligand.

The parameter $\log_{10} X$ (eqns. 7 and 8), may be employed in mixed ligand complexes for stability quantification purposes
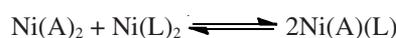
$$Ni(A)_2 + Ni(L)_2 \rightleftharpoons 2Ni(A)(L)$$

$$X_{Ni(A)(L)} = \frac{[Ni(A)(L)]^2}{[Ni(A)_2][Ni(L)_2]} \quad (7)$$

$$\log_{10} X_{Ni(A)(L)} = 2\log_{10} \beta_{Ni(A)(L)} - (\log_{10} \beta_{Ni(A)_2} + \log_{10} \beta_{Ni(L)_2}) \quad (8)$$

Similar conclusions are achieved by $\log_{10} X$ and $\Delta\log_{10} K$. Statistically [25], the stability of mixed complexes was reinforced by the more positive values of $\log_{10} X$ obtained. Moreover, positive values are considered as evidence of enhanced stability as a result of intermolecular ligand-ligand interactions, hydrogen bonding, the π-back donation effect and/or hydrophobic effects. The speciation diagram of histidine complexes, which are considered as representatives of amino acid (Fig. 1). The complex species of [Ni(A)(His)] achieve 33% of maximum concentration at the pH value of 8.6. Thus, it is predominant in the range of physiological pH.

Solid state measurements: The molar conductance values of two nickel(II) chelates which are observed at 2.36 and 4.82 Ω^{-1} cm^2 mol^{-1}. These values suggest non-electrolyte nature of the present complexes [26]. Chelates **1** and **2** do not possess any crystallographically imposed symmetry. The mass spectrum of two nickel(II) chelates were affected by the electron (Fig. 2) confirmed the suggested formula by showing the peak at 268.8

TABLE-1
STABILITY CONSTANTS OF THE TERNARY SPECIES IN THE Ni(II)-A-L SYSTEMS AND
PROTON-ASSOCIATION CONSTANTS AND THEIR BINARY STABILITY CONSTANTS

Systems	1	p	q	r^a	$\log_{10} \beta^b$	$\log_{10} K_{Ni(A)(L)}^{Ni(A)}$	$\log_{10} K_{Ni(A)(L)}^{Ni(L)}$	$\log_{10} X$
5-Aminolevulinic acid (A)	0	0	1	1	9.73 (0.01)	–	–	–
	0	0	1	2	11.98 (0.01)			
	1	1	0	0	5.65 (0.01)			
	1	2	0	0	13.22 (0.02)			
L-Alanine (Ala)	0	0	1	1	9.62 (0.01)	9.88	8.10	3.65
	0	0	1	2	11.81 (0.02)			
	1	0	1	0	7.89 (0.01)			
	1	0	2	0	13.61 (0.01)			
	1	1	1	0	15.24 (0.07)			
Valine (Val)	0	0	1	1	9.57 (0.02)	9.47	7.96	2.93
	0	0	1	2	11.70 (0.01)			
	1	0	1	0	7.16 (0.02)			
	1	0	2	0	14.09 (0.02)			
	1	1	1	0	15.12 (0.02)			
Serine (Ser)	0	0	1	1	9.15 (0.02)	9.39	7.83	3.46
	0	0	1	2	11.35 (0.01)			
	1	0	1	0	7.21 (0.01)			
	1	0	2	0	13.40 (0.02)			
	1	1	1	0	15.04 (0.01)			
Methylamine (Met)	0	0	1	1	10.55 (0.01)	3.58	5.06	-2.36
	1	0	1	0	4.17 (0.02)			
	1	0	2	0	7.60 (0.05)			
	1	1	1	0	9.23 (0.01)			
	1	1	2	0	13.57 (0.01)			
Imidazole (Imi)	0	0	1	1	7.26 (0.01)	2.53	4.17	-4.06
	1	0	1	0	4.01 (0.02)			
	1	0	2	0	7.20 (0.05)			
	1	1	1	0	8.18 (0.01)			
	1	1	2	0	10.43 (0.01)			
Histidine (His)	0	0	1	1	9.53 (0.01)	11.92	9.76	3.81
	0	0	1	2	15.81 (0.03)			
	1	0	1	0	7.81 (0.01)			
	1	0	2	0	18.11 (0.01)			
	1	1	1	0	17.57 (0.03)			
	1	1	1	1	24.82 (0.01)			
Cysteine (Cys)	0	0	1	1	9.78 (0.01)	12.66	9.33	3.37
	0	0	1	2	17.67 (0.05)			
	1	0	1	0	8.98 (0.01)			
	1	0	2	0	20.03 (0.01)			
	1	1	1	0	18.31 (0.01)			
	1	1	1	1	25.74 (0.01)			
Penicillamine (Pen)	0	0	1	1	10.12 (0.01)	13.87	8.07	3.69
	0	0	1	2	17.97 (0.02)			
	1	0	1	0	11.45 (0.01)			
	1	0	2	0	22.13 (0.02)			
	1	1	1	0	19.52 (0.01)			
	1	1	1	1	24.60 (0.01)			

The stoichiometric coefficients ^{a}p, r, q and l correspond to A, H^+, amino acids and Ni(II), in order. ^{b} Standard deviations are given in parentheses.
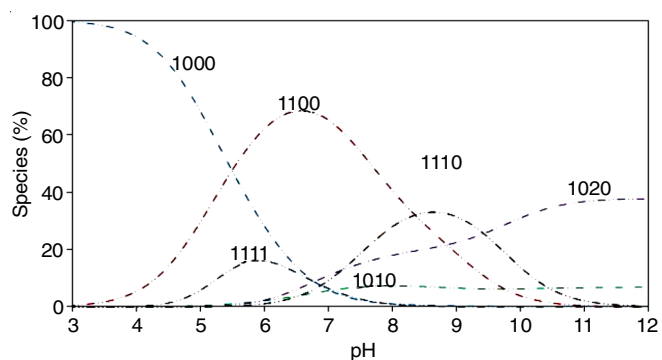
Fig. 1. Percentage distribution curves of mixed ligand Ni(II)-A-His system

and 309.0 amu corresponding to the two nickel(II) chelates moieties ($C_5H_{10}N_2O_7Ni$) and ($C_8H_{14}N_2O_5SNi$) atomic mass 268.8 and 309.0 amu, respectively.

NMR analysis: No signals that correspond to alcoholic and primary amine protons were detected in the ^{1}H NMR spectra of the nickel(II) chelates in CDCl$_3$. On the other hand, at δ 8.58 ppm, a multiplet that corresponds to amide HNC=O, 4H protons are shown. However, signals that correspond to alcoholic and primary amine protons are not shown. Conversely, an observation of a multiplet signal corresponding to methylene proton CH$_2$ was made, 6H for chelate **1** and 2H for chelate **2** that are adjacent to the nitrogen atom appeared at δ 3.45 and
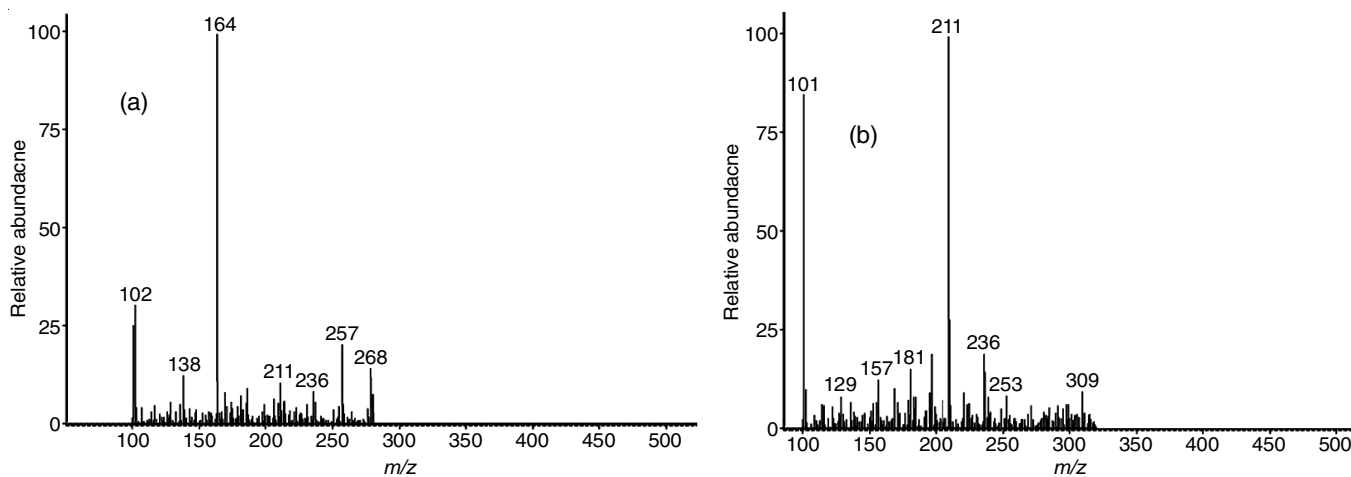
Fig. 2. Mass spectra of chelates **1** and **2**

3.42 ppm. NMR spectrum also shows a singlet at δ 2.33 ppm corresponding to CO-CH₂-S, 8H which is close to sulphur atom.

In ¹H NMR spectra of chelates **1** and **2**, methylene groups′ protons were deshielded due to the presence of nitrogen and oxygen atoms and were observed in the range of δ 2.20-3.06 ppm. Secondary amine and carboxyl protons were also deshielded due to the presence of adjacent electronegative nitrogen and oxygen atoms and appeared as singlet at δ 1.52 and 10.43 ppm for imine and carboxyl groups, respectively in chelate **1**. Signal methylene, amino and thiol groups protons for cysteine (Cys) were observed at δ 3.84, 1.53, 12.23 and 10.42 ppm, respectively in chelate **2** [27].

IR analysis: No bands that correspond to the free primary diamine were displayed by the IR specta of nickel(II) chelates [28]. Four new bands were shown in the spectra of nickel(II) chelates in the regions: 780, 1248, 1590 and 1620 cm⁻¹ and they correspond to amide IV [δ(C=O)], amide III [δ(N-H)], amide II [ν(C-N) + δ(N-H)] and amide I [ν(C=O)] bands, in the order given [29,30]. The bands observed at ~795 and 1478 cm⁻¹ may be assignable to thioamides I and II, respectively. The sharp band seen at ~3278 cm⁻¹ could be due to [ν(N-H)] of the secondary amino group [31]. IR spectrum of nitrate chelate **1** displays three (N-O) stretching bands, at 1436 cm⁻¹ (ν₅), 1312 cm⁻¹ (ν₁) and 1023 cm⁻¹ (ν₂). The separation of two highest frequency bands (ν₅–ν₁), Δ is 124 cm⁻¹. Suggesting that the nitrate group is coordinated to the central metal ion [32] in unidentate manner.

Thermal analysis: The thermal analysis curves of the complexes are given in Fig. 3. The thermal decomposition of the complexes proceeds in three stages. The Ni(II) chelates are thermally stable up to 130 and 140 ℃, respectively. The first stage of decomposition corresponding to endothermic dehydration of chelate **1** by the loss of one water molecule occurs in the temperature range 130-200 ℃, respectively. The intermediates formed are stable up to 310 and 265 ℃. The second decomposition with exothermic peak by the loss of ligands (A and L) moieties occurs in the temperature range 310-550 ℃ and 260-640 ℃. The solid residues above 665 and 680 ℃ were identified as NiO.
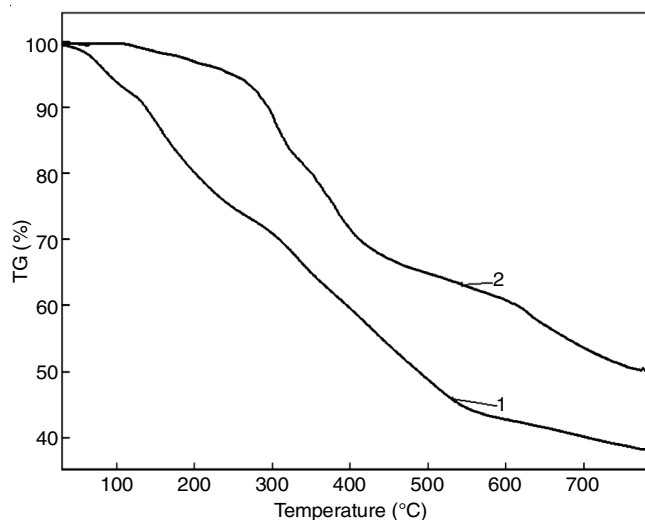
Fig. 3. TG curves of chelates **1** and **2**

Magnetic moment: At room temperature, Ni(II) chelates behave diamagnetically, which implies that the surrounding environment of Ni(II) ion is a square-planar environment. Moreover, the observed three bands of absorption of the two Ni(II) chelates in the electronic spectra are in the range 14,048 and 14,248 (ε = 239 and 322 mol⁻¹ cm⁻¹), 20,442 and 21,003 (ε = 82 and 88 mol⁻¹ cm⁻¹), and 23,108 and 23,576 cm⁻¹ (ε = 123 and 133 mol⁻¹ cm⁻¹) corresponding to square planner geometry [33]. These bands may be assigned to the three spin allowed transitions: ¹A₁g(D) → ¹A₂g(G) (ν₁), ¹A₁g(D) → ¹B₂g(G) (ν₂) and ¹A₁g(D) → ¹Eg(G) (ν₃), respectively [33].

CONFLICT OF INTEREST

The authors declare that there is no conflict of interests regarding the publication of this article.

REFERENCES

1. S.J. Heater, M.W. Carrano, D. Rains, R.B. Walter, D. Ji, Q. Yan, R.S. Czernuszewicz and C.J. Carrano, *Inorg. Chem.*, **39**, 3881 (2000); https://doi.org/10.1021/ic000389r

2. J.T.H. Roos and D.R. Williams, *J. Inorg. Nucl. Chem.*, **39**, 1294 (1977); https://doi.org/10.1016/0022-1902(77)80373-4

3. N.B. Behrens, G.M. Diaz and D.M.L. Goodgame, *Inorg. Chim. Acta*, **125**, 21 (1986); https://doi.org/10.1016/S0020-1693(00)85478-X

4. A. Cole, J. Goodfield, D.R. Williams and J.M. Midgley, *Inorg. Chim. Acta*, **92**, 91 (1984); https://doi.org/10.1016/S0020-1693(00)80004-3

5. R.S. Srivastava, *Inorg. Chim. Acta*, **55**, 71 (1981); https://doi.org/10.1016/S0020-1693(00)90772-2

6. H.A. Azab, A. Hassan, A.M. El-Nady and R.S.A. Azkal, *Monatsh. Chem.*, **124**, 267 (1993); https://doi.org/10.1007/BF00810582

7. M. Taha and M.M. Khalil, *J. Chem. Eng. Data*, **50**, 157 (2005); https://doi.org/10.1021/je049766v

8. M.F. Charlot, O. Kahn, S. Jeannin and Y. Jeannin, *Inorg. Chem.*, **19**, 1410 (1980); https://doi.org/10.1021/ic50207a068

9. H. Sigel, B.P. Operschall, S.S. Massoud, B. Song and R. Griesser, *Dalton Trans.*, 5521 (2006); https://doi.org/10.1039/b610082a

10. D. Czakis-Sulikowska, A. Czylkowska, J. Radwanska-Doczekalska, R. Grodzki and E. Wojciechowska, *J. Therm. Anal. Calorim.*, **90**, 557 (2007); https://doi.org/10.1007/s10973-006-7980-9

11. J.R. Bocarsly and J.K. Barton, *Inorg. Chem.*, **31**, 2827 (1992); https://doi.org/10.1021/ic00039a030

12. O. Farver and I. Pecht, *Coord. Chem. Rev.*, **94**, 17 (1989); https://doi.org/10.1016/0010-8545(89)80043-8

13. J. Crowe, H. Dobeli, R. Gentz, E. Hochuli, D. Stuber and K. Henco, *Methods Mol. Biol.*, **31**, 371 (1994); https://doi.org/10.1385/0-89603-258-2:371

14. L. Nieba, S.E. Nieba-Axmann, A. Persson, M. Hämäläinen, F. Edebratt, A. Hansson, J. Lidholm, K. Magnusson, Å.F. Karlsson and A. Plückthun, *Anal. Biochem.*, **252**, 217 (1997); https://doi.org/10.1006/abio.1997.2326

15. K.M. Maloney, D.R. Shnek, D.Y. Sasaki and F.H. Arnold, *Chem. Biol.*, **3**, 185 (1996); https://doi.org/10.1016/S1074-5521(96)90261-6

16. Y. Morokuma, M. Yamazaki, T. Maeda, I. Yoshino, M. Ishizuka, T. Tanaka, Y. Ito and R. Tsuboi, *Int. J. Dermatol.*, **47**, 1298 (2008); https://doi.org/10.1111/j.1365-4632.2008.03783.x

17. H. Rossotti, Chemical Applications of Potentiometry, Van Mostrand: London, U.K. (1968).

18. G. Gran, *Acta Chem. Scand.*, **4**, 559 (1950); https://doi.org/10.3891/acta.chem.scand.04-0559

19. P. Gans, A. Sabatini and A. Vacca, *Talanta*, **43**, 1739 (1996); https://doi.org/10.1016/0039-9140(96)01958-3

20. L. Alderighi, P. Gans, A. Ienco, D. Peters, A. Sabatini and A. Vacca, *Coord. Chem. Rev.*, **184**, 311 (1999); https://doi.org/10.1016/S0010-8545(98)00260-4

21. H.D. Demir, M. Pekin, A.K. C¨uc¨u, E. D¨olen and H.Y. Aboul-Enein, *Toxicol. Environ. Chem.*, **71**, 357 (1999); https://doi.org/10.1080/02772249909358806

22. W. Sang-Aroon and V. Ruangpornvisuti, *Int. J. Quantum Chem.*, **108**, 1181 (2008); https://doi.org/10.1002/qua.21569

23. S.A.A. Sajadi, *Nat. Sci.*, **2**, 85 (2010); https://doi.org/10.4236/ns.2010.22013

24. W. Kadima and D.L. Rabenstein, *J. Inorg. Biochem.*, **38**, 277 (1990); https://doi.org/10.1016/0162-0134(90)80003-G

25. H. Sigel, Metal Ions in Biological Systems, Marcel Dekker: New York vol. 2 (1973).

26. I.J. Kang, L.W. Wang, T.A. Hsu, A. Yueh, C.-C. Lee, Y.-C. Lee, C.-Y. Lee, Y.-S. Chao, S.-R. Shih and J.-H. Chern, *Bioorg. Med. Chem. Lett.*, **21**, 1948 (2011); https://doi.org/10.1016/j.bmcl.2011.02.037

27. P. Nath, M.K. Bharty, B. Maiti, A. Bharti, R.J. Butcher, J.L. Wikaira and N.K. Singh, *RSC Adv.*, **6**, 93867 (2016); https://doi.org/10.1039/C6RA15186H

28. S. Chandra, S.D. Sharma and U. Kumar, *Synth. React. Inorg. Met.-Org. Chem.*, **34**, 79 (2004); https://doi.org/10.1081/SIM-120027318

29. S. Chandra and L.K. Gupta, *Transition Met. Chem.*, **27**, 196 (2002); https://doi.org/10.1023/A:1013935602736

30. S. Chandra and L.K. Gupta, *J. Saudi Chem. Soc.*, **7**, 243 (2003).

31. M. Shakir, S.P. Varkey and P.S. Hameed, *Polyhedron*, **12**, 2775 (1993); https://doi.org/10.1016/S0277-5387(00)80058-3

32. K. Nakamoto, Infrared Spectra of Inorganic and Coordination Compounds, Wiley Interscience: New York (1970).

33. A.B.P. Lever, Crystal Field Spectra. Inorganic Electronic Spectroscopy, Elsevier: Amsterdam, edn 1 (1968).